High-Strength and High-Toughness Polyimide Nanofibers: Synthesis and Characterization

Chuyun Cheng,[1] Juan Chen,[1] Fei Chen,[1] Ping Hu,[1] Xiang-Fa Wu,[2] Darrell H. Reneker,[3] Haoqing Hou[1]

[1]*Chemistry Institute of Jiangxi Normal University, Nanchang 330027, China*
[2]*Department of Mechanical Engineering and Applied Mechanics, North Dakota State University, Fargo, North Dakota 58108-6050*
[3]*Department of Polymer Science, University of Akron, Akron, Ohio 44325*

Received 5 February 2009; accepted 7 September 2009
DOI 10.1002/app.31523
Published online 5 January 2010 in Wiley InterScience (www.interscience.wiley.com).

ABSTRACT: High-strength and high-toughness nanofibers were made from polyimide 6F-PI through electrospinning. The 6F-PI had a backbone made up with 3,3′,4,4′-biphenyl-tetracarboxylic dianhydride and 2,2-bis[4-(4-aminophenoxy)phenyl]-hexafluoro-propane residues. Electrospun 6F-PI precursor nanofibers were collected in the form of aligned fiber sheet on the rim of a rotating disc. Heating process converted the precursor fiber sheets to 6F-PI nanofiber sheets. Gel permeation chromatography and Ostwald Viscometer were used to determine the molecular weight and the molecular weight distribution of the 6F-PI precursor, i.e., the 6F-polyamic acid. Scanning electron microscopy, infrared spectroscopy, X-ray scattering, tensile testing, dynamic mechanical analysis, thermogravimetric analysis, and differential scanning calorimetry were employed to characterize the surface morphology, thermal stability, and mechanical properties of the 6F-PI nanofiber sheets. Experimental results show that the nanofibers were well aligned in the sheets with fiber diameters ranging from 50 to 300 nm. The nanofiber sheets were stable to over 450°C, with a glass transition at 265.2°C. The uniaxial tension test showed that the 6F-PI nanofiber sheets had superior mechanical properties. The ultimate tensile strength, modulus, toughness, and elongation to break of the 6F-PI nanofiber sheets are respectively, 308 ± 14 MPa, 2.08 ± 0.25 GPa, 365 ± 20 MPa, and 202 ± 7%. It is expected that electrospun PI nanofibers with such high toughness and high ultimate tensile strength can find applications in high-performance textiles and composites, for example. J Appl Polym Sci 116: 1581–1586, 2010

Key words: polyimide; electrospun nanofibers; high elongation; high toughness

INTRODUCTION

Polyimides form a well-known class of polymer materials with excellent thermal behavior and mechanical properties and very good chemical resistance and electrical properties. Because of these outstanding properties, polyimides have found extensive applications as fibers,[1–4] films,[5–8] coatings,[9–11] photoresists,[12–15] and composites,[16–20] for many years. Ultra-thin polyimide fibers can be made with nanometer scale diameters by means of electrospinning.[21–23] It was found that the electrospun polyimide nanofibers had remarkably better mechanical properties than those made of other polymer, such as polyacrylonitrile (PAN), nylon, Nomex, polylactide (PLA), and the like. For instance, the mats of partially aligned polyimide nanofibers based on 4,4′-Biphenyltetracarboxylic dianhydride (BPDA)/p-phenylenediamine (PPA) had an average tensile strength of 660 MPa, Young's modulus of 16 GPa, and 5% elongation to break[21]; however, the constituent single polyimide nanofibers had an average tensile strength of 1.7 GPa, Young's modulus of 80 GPa and 3% elongation to break.[22] To enhance their compliance, polyimide copolymer nanofibers were produced based on BPDA/BPA/ODA (mole ratio = 100/40/60). The resulting copolymer nanofibers had an average strength of 1.1 GPa, Young's modulus of 15 GPa, and an elongation to break about 20%, measured on a belt of aligned nanofibers.[23] Although the improved elongation to break of the polyimide copolymer nanofibers was almost fourfold higher than that of the BPDA/PPA polyimide nanofibers reported previously,[21,23] the absolute magnitude is still relatively low by comparison with many polymer fibers. In view of strain energy and solid mechanics, lower elongation corresponds to lower toughness and impact resistance.

Therefore, in this work, we developed an experimental scheme to synthesize a novel polyimide with

Correspondence to: H. Hou (haoqing@jxnu.edu.cn).
Contract grant sponsor: Ministry of Education of PRC; contract grant number: 707038.
Contract grant sponsor: Jiangxi Provincial Department of Science and Technology; contract grant number: 050008.
Contract grant sponsor: NSFC; contract grant numbers: 20674034, 20874041.

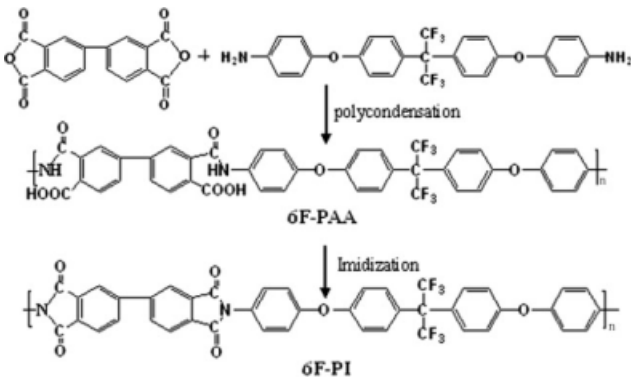

Figure 1 Reaction equations of polycondensation and imidization of the polymers.

a flexible diamine, 2,2-bis[4-(4-aminophenoxy)phenyl]hexafluoropropane (6F-BAPP) as one of the monomers, which was usually used to synthesize organosoluble polyimides or low dielectric constant polyimides because of its flexibility.[24–26] The resulting polyimide nanofibers have both high strength and high elongation to break. As the three-sp^3 elements (2O, 1C) that form sp^3 bonds exist on the polymer backbone, which separates the rigidity of the aromatic rings, the resulting polyimide with the flexible diamine residue was expected to increase the nanofiber elongation. As expected, the nanofiber sheets made from the flexible polyimide had an elongation-to-break over 200%, which is 40-fold the strain of BPDA/PPA polyimide nanofiber sheets reported in the literature.[21] The corresponding tensile strength is beyond 300 MPa and the toughness is over 360 MPa.

EXPERIMENTAL

Materials

N,*N*-dimethyl acetamide (DMAc) (Jinwei Chem Co., Shanghai, China) was distilled over P_2O_5 under reduced pressure. BPDA (Jida Plastic Products Co., Hebei, China) was purified by sublimation before use. 6F-BAPP was synthesized described as previous work.[27] Dodecylethyldimethylammonium bromide (DEDAB, 98%, Aldrich) was used as received.

Synthesis of PI precursor 6F-PAA

Equi-molar amounts of BPDA (2.9423 g, 0.01 mol), 6F-BAPP (5.1846 g, 0.01 mol), and 73.0 g DMAc were mixed in a 250 mL four-necked flask equipped with a mechanical stirrer, thermometer, nitrogen inlet, and outlet, followed by intense mechanical stirring at 0–1°C for 48 h. The equation of the polycondensation was schematized as shown in Figure 1. The concentration of the as-synthesized polyamic acid (6F-PAA) in DMAc was 10% by weight. The mixture resulted in a highly viscous polymer solution. The intrinsic viscosity of the 6F-PAA was measured to be 5.40 dL/g in DMAc.

Fabrication of aligned nanofiber sheets

The electrospinning process was performed on a solution of the above precursor in DMAc. A small amount of DEDAB was added to increase the electrical conductivity of the solution for electrospinning. The parameters of the solution adopted for electrospinning were listed in Table I. The average electrical field was on the order of 200 kV/m, which was triggered by introducing a 50 kV electrical potential into a 25 cm gap from the spinneret to a drum-shaped collector (with diameter around 0.28 m), which rotated at a preset speed. The as-electrospun 6F-PAA nanofibers were collected as a sheet of aligned nanofibers on the rotation drum.

Imidization of nanofiber sheets

Imidization of the nanofiber sheets was implemented within a tubular glass reactor at temperatures ranging from room temperature to 250°C, in vacuum. This process follows the protocol: (1) holding at 100°C in vacuum for 2 h to remove the residual solvent; (2) heating up to 160°C at a rate of 10°C/min and annealing for 15 min; (3) heating up to 200°C at a rate of 5°C/min and annealing for 15 min; (4) heating up to 250°C at a rate of 3°C/min and annealing for 60 min to complete the imidization process.

Characterization

Infrared spectra of the PAA and PI nanofiber sheet samples were recorded by using a Bruker Tensor 27 spectrophotometer in the transmission mode. Wide-angle X-ray diffraction was carried out using a BEDE D1 system with Cu-α radiation. Images of the nanofibers and the nanofiber sheets were captured by using a Quanta 200 scanning electron microscope (SEM). Mechanical properties of the PI nanofiber sheets were characterized through uniaxial tension

TABLE I
Parameters of the Solution for Electrospinning

Sample	Concentration of 6F-PAA (wt %)	Concentration of DEMAB (wt %)	Viscosity (Pa.s)	Electrical conductivity (μS/cm)
Solution for electrospinning	3.0	0.12	5.92	51.0

TABLE II
Intrinsic Viscosity, Molecular Weight, and Molecular Weight Distribution of 6-F-PAA

Sample	[η](dL/g)	M_w	M_n	M_w/M_n
6F-PAA	5.40	8.3×10^5	5.2×10^5	1.6

tests on an electromechanical universal testing machine (Model: CMT-8102, SANS company). All the tension tests were performed under the displacement-control mode at the constant cross-head speed of 5 mm/min. The samples for tensile testing were 2 mm in width and 60 mm in length. The thickness of the sample was calculated based on the sample weight and density of corresponding PI. For example, the weight of a piece of the PI nanofiber sheet of 60 × 10 mm^2 was 12.8 mg and the density of the PI was 1.39 g/cm^3, which was determined from the weight and volume of the corresponding film. The thickness of the aligned 6F-PI nanofiber sheet was 15.3 μm.

Thermal stability analysis of the nanofibers was carried out on a thermogravimetric analyzer WRT-3P (Shanghai) at a heating rate of 10°C/min in air. Differential scanning calorimetric (DSC) measurement was conducted on the nanofiber sheet sample, using a Netzsch DSC 200F3, in standard aluminum pans, with a heating and cooling rate of 10°C/min. The dynamic mechanical analysis (DMA) of the nanofiber sheets was performed using a Perkin–Elmer Pyris diamond DMA at a heating rate of 3°C/min in nitrogen. The frequency and amplitude utilized for the characterization were respectively, 1 Hz and 20 μm; and the fiber alignment direction in the sample was along the stretching direction. The storage modulus (E′), loss modulus (E″), and loss tangent (tanδ) of the nanofiber sheets were recorded in the temperature range from 20 to 350°C. Intrinsic viscosity of the 6F-PI precursor, 6F-PAA, was measured using an Ostwald Viscometer, and the solvent was DMAc, at 25°C. Gel permeation chromatography was carried out using a Waters 1515 system with a polystyrene standard for calibration. The viscosity and electrical conductivity of the concentrated 6F-PAA-solution in DMAc were measured respectively, using a NDJ-8S digital viscometer (Shanghai Precision and Scientific Instrument Co) and a DDS-11D conductivity meter (Shanghai Precision and Scientific Instrument Co).

RESULTS AND DISCUSSIONS

Synthesis of 6F-PI precursor

BPDA is a highly active dianhydide and 6F-BAPP is a highly active diamine. As a result, the polycondensation between dianhydride and diamine is rapid in an aprotic solvent such as DMAc. However, a higher reactivity, for a polymerization, often means a lower molecular weight and a broader molecular-weight distribution. To form a polymer product with a high molecular weight and a narrow molecular-weight distribution, the polycondensation of BPDA and 6F-BAPP was performed at a lower temperature from 0 to 1°C, for 48 h. The polymerization resulted in a highly viscous 6F-PAA solution in DMAc. To enhance the reaction, intense mechanical stirring is needed due to the high viscosity of the reaction mixture. The intrinsic viscosity, molecular weight, and molecular weight distribution of the as-synthesized polyamic acids were listed in Table II. The high molecular weight of 8.3×10^5 Dalton and the narrow molecular weight distribution is desirable for producing high performance nanofibers.

Formation of aligned 6F-PI nanofiber sheets

Aligned nanofiber sheets were fabricated with aid of a rotating disc or drum that served as the fiber collector.[21,23,28] In this study, the 6F-PAA nanofibers were assembled at the rim of a disc rotating at a surface speed of 24 m/s. Figure 2 shows the alignment

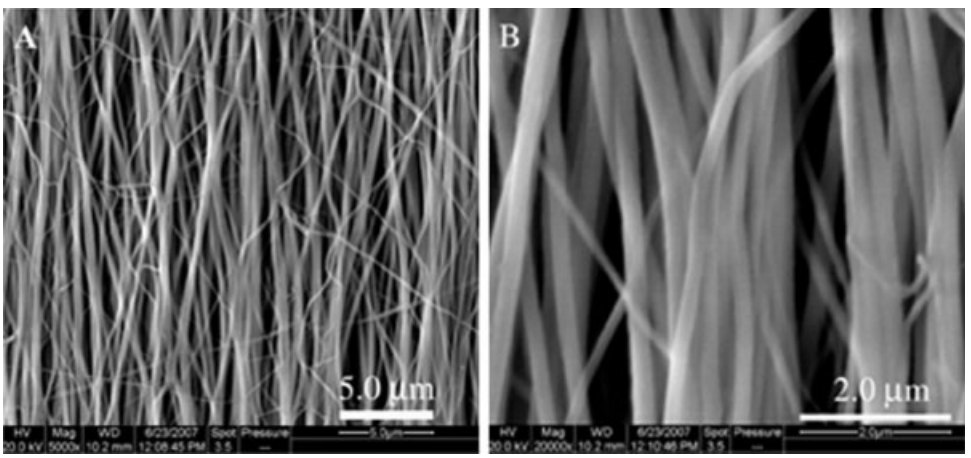

Figure 2 Typical SEM images of aligned 6F-PI nanofiber sheet: low magnification (A) and high magnification (B).

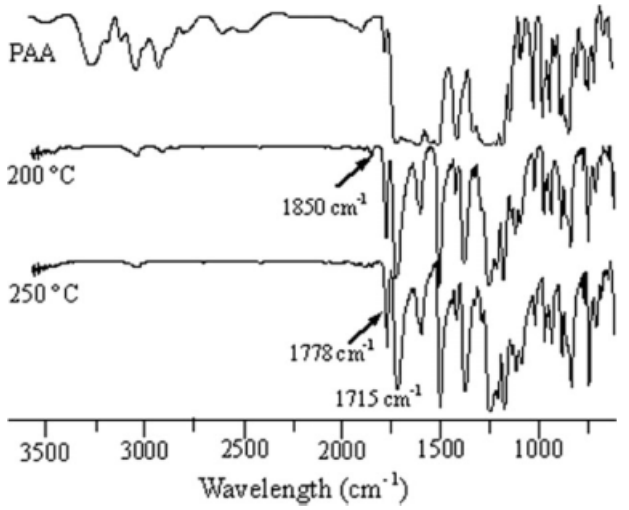

Figure 3 FT-IR spectra of typical 6F-PI and 6F-PAA.

of fiber along the rotating direction. The alignment degree of the nanofibers in sheets is about 85%, determined by counting the fraction of fibers with almost the same stretching direction in the SEM image. Though the fiber diameter was in the range from 50 to 300 nm, most of diameters were in the range of 150–250 nm. The PI nanofibers were formed from the above precursor nanofibers by imidization at high temperature, as described in Section 2. IR spectra showed that the imidization of 6F-PAA was almost completed at 200°C (Fig. 3). A small peak at 1850 cm^{-1} was detected, which can be attributed to the stretching vibrations of C=O in an anhydride group —CO—O—CO—, which was formed as one of the end groups of a polymer molecule in the course of imidization due to an inner reaction of adjacent carboxy and amido groups. This is the reverse reaction of polycondensation between dianhydride and diamine. Upon heating to 250°C, the small peak disappeared, due to a further reaction between the end groups.

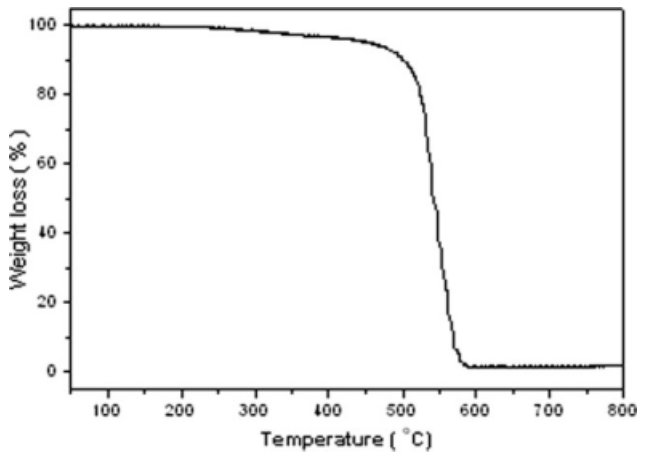

Figure 4 TGA curve of a typical 6F-PI nanofiber sheet.

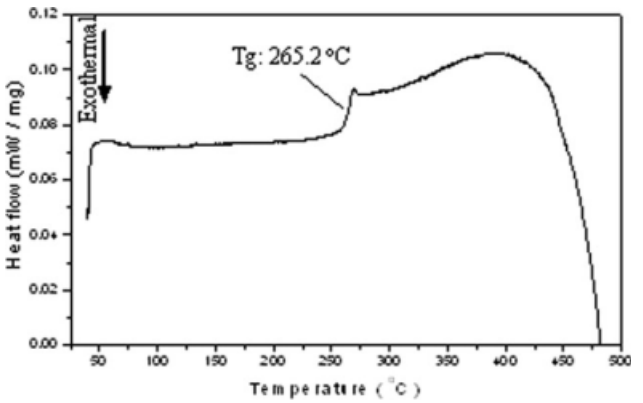

Figure 5 DSC curve of a typical aligned 6F-PI nanofiber sheet.

Thermal properties of 6F-PI nanofibers

Although flexible diamine residues were involved, the 6F-PI molecules still sustain a high thermal stability. The thermogravimetric analyses of the electrospun 6F-PI nanofiber sheets are shown in Figure 4. It was found that the 6F-PI nanofiber samples obtained at imidization temperature of 250°C had a thermal stability temperature beyond 450°C, and the glass transition temperature of the 6F-PI nanofibers did not decrease, either. Figure 5 shows a DSC heating diagram for a typical nanofiber sheet sample. The glass transition temperature is 265.2°C, but no clear crystallization or melting signals are detected on the DSC curve, below the decomposition temperature of 450°C. The DMA behavior of a typical 6F-PI nanofiber sheet is illustrated in Figure 6. The strong and sharp peak on Curve 2 indicates that the 6F-PI nanofiber sheet, imidized at 250°C, had a prominent α transition around 262°C, which is correlated to the T_g of 6F-PI nanofibers. The storage modulus decreased gradually from 3.5 to 2.0 GPa in the temperature range from 50 to 250°C, and decreased abruptly from 2.0 to ~ 15 MPa at ~ 260°C (curve 1).

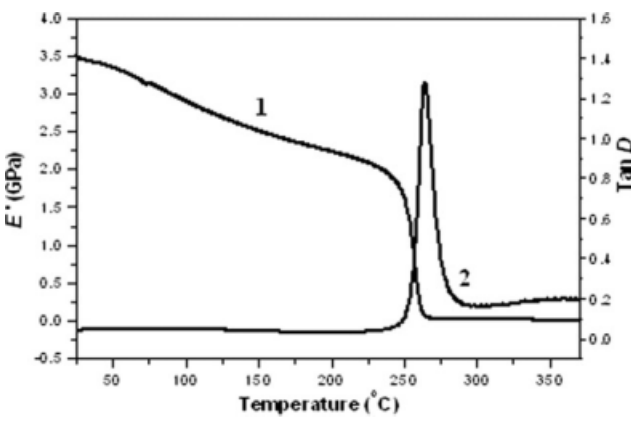

Figure 6 Tan(δ) curves of typical electrospun PI nanofiber belts with different imidization temperature.

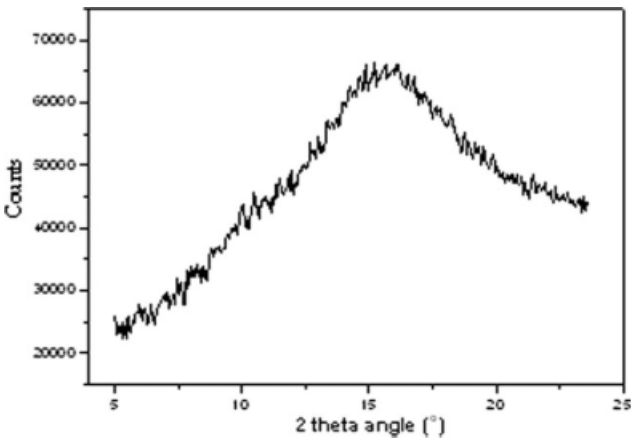

Figure 7 Wide angle X-ray scattering diagram of a typical aligned 6F-PI nanofiber sheet.

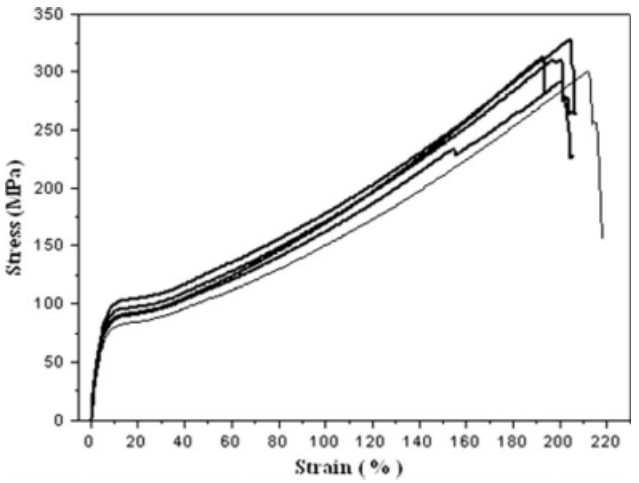

Figure 8 Typical stress–strain curves of electrospun 6F-PI nanofibers sheets.

According to the above DSC analysis and the dynamic mechanical behavior of the 6F-PI nanofiber sheet, we conclude that the polymer in the nanofibers is amorphous. This is further confirmed by X-ray diffractions (Fig. 7). An amorphous halo was observed at a scattering angle of $2\theta = 16°$.

Mechanical properties of 6F-PI nanofiber sheets

The tensile test results are tabulated in Table III. Typical stress–strain curves are shown in Figure 8. The tensile behavior of the aligned nanofiber sheet is quite different from that previously reported by the present authors.[21,23] The 6F-PI nanofiber sheet has a yield at the strain of $\sim$ 10%, then hardened with the increase of stress as the stretching increased, to a strain of up to 200%. Such a tensile behavior is unusual for a PI fiber sample. The high molecular weight and flexible backbone structure of the 6F-PI might be responsible for such a high strain and long hardening stage. Due to the ultra-high elongation to break, the 6F-PI nanofiber sheet has a toughness of 365 MPa, which is an unusual high value among the previously reported textile polyimide fibers and electrospun polyimide nanofibers.

TABLE III
Mechanical Properties of Aligned 6F-PI Nanofiber Sheets

Sample	Tensile strength (MPa)	Young's modulus (GPa)	Strain (%)	Toughness (MPa)
1	299	2.44	211.5	367
2	327	1.96	204.4	392
3	291	1.98	200.0	355
4	310	2.24	200.5	374
5	313	1.80	193.0	338
Average	308 ± 14	2.08 ± 0.25	201.9 ± 6.8	365 ± 20

CONCLUSIONS

High strength and high toughness sheets of aligned nanofibers were produced from 6F-PI (based on BPDA/6F-BAPP) by electrospinning. The flexible diamine 6F-BAPP residues decreased the rigidity of the 6F-PI backbone and its crystallinity. The 6F-PI was in the amorphous state after electrospinning according to the analyses based on DSC, DMA, and X-ray diffraction. Meanwhile, the toughness of the nanofiber sheet was as much as 365 MPa, among the highest of common polymer materials. The nanofiber sheets have excellent thermal stability, with the T_g beyond 265°C and decomposition temperature at 450°C. Such nanofibers have a promising future in making heat-resistant filters, and impact-resistant protective clothes, for example.

References

1. Kanada, T.; Katsura, T.; Nakagawa, K.; Makino, H.; Horio, M. J Appl Polym Sci 1986, 32, 3151.
2. Kanada, T.; Katsura, T.; Nakagawa, K.; Makino, H.; Horio, M. J Appl Polym Sci 1986, 32, 3133.
3. Park, S. K.; Farris, R. J. Polymer 2002, 42, 10087.
4. Mihailov, G. M.; Lebejeva, M. F.; Baklagina, Y. G.; Maricheva, T. A. J Pract Chem (Russ) 2000, 73, 472.
5. Ghosh, M. K.; Mittal, K. L., Eds. Polyimides: Fundamentals and Applications; Marcel Dekker: New York, 1996.
6. Dine-Hart, R. A.; Wright, W. W. J Appl Polym Sci 1967, 11, 609.
7. Endrey, A. L. U.S. Pat. 3,197,630 (1965).
8. Itatani, H.; Inaike, T.; Yamamoto, S. U. S. Pat. 4,568,715 (1986).
9. Takahashi, Y.; Iijima, M.; Oishi, Y.; Kakimoto, M. A.; Imai, Y. Macromolecules 1991, 24, 3543.
10. Yamamoto, T.; Takahashi, T.; Narui, K.; Mitsui, H.; Komoda, N. U.S. Pat. 6,548,180 (2003).
11. Chung, H.; Loe, Y.; Han, H. J Appl Polym Sci 1999, 74, 3287.
12. Minnema, L.; Van der Zande, J. M. Polym Eng Sci 1988, 28, 815.
13. Higuchi, H.; Yamashita, T.; Horie, K.; Mita, I. Chem Mater 1991, 3, 189.

14. Watanabe, Y.; Fukukawa, K. I.; Shibasaki, Y.; Ueda, M. J Polym Sci Part A: Polym Chem 2005, 43, 593.
15. Hou, H.; Jiang, J.; Ding, M. Eur Polym J 1999, 35, 1993.
16. Hou, T. H.; St Clair, T. L. High Perform Polym 1998, 10, 193.
17. Connell, J. W.; Smith, J. G., Jr.; Hergenrother, P. M.; Romme, M. L. High Perform Polym 2000, 12, 323.
18. Hedrick, J. L.; Labadie, J. W.; Russell, T.; Wakharkar, V. Polymer 1993, 34, 122.
19. Carter, K. R.; Di Pietro, R.; Sanchez, M. I.; Russell, T. P.; Lakshmanan, P.; McGrath, J. E. Chem Mater 1997, 9, 105.
20. Chu, Q. H.; Zhang, J.; Xu, Z. Y.; Ding, M. X. Macromol chem Phys 2000, 201, 505.
21. Huang, C. B.; Chen, S. L.; Reneker, D. H.; Lai, C. L.; Hou, H. Adv Mater 2006, 18, 668.
22. Chen, F.; Peng, X.; Li, T.; Chen, S.; Wu, X. F.; Reneker D. H.; Hou, H. J Phys Appl Phys 2008, 41:025308.
23. Chen, S.; Hu, P.; Greiner, A.; Cheng, C.; Cheng, H.; Chen, F. F.; Hou, H. Nanotechnology 2008, 19, 015604.
24. Eci, Y. I.; Kawamura, I. C. O.; Giwara, T.; Takahashi, Y.; Suzuki, Y. I.; Kimoto, M. I.; Mai, Y. J Polym Sci Part A Polym Chem 1992, 30, 2281.
25. Liaw, D. J.; Wang, K. L. J Polym Sci Part A Polym Chem 1996, 34, 1209.
26. Bruma, M.; Schulz, B.; Mercer, F. W. Polymer 1994, 35, 4209.
27. Sato, M.; Yokoyama, M. Eur Polym J 1979, 15, 733.
28. Hou, H.; Ge, J. J.; Zeng, J.; Li, Q.; Reneker, D. H.; Greiner, A.; Cheng, S. Z. D. Chem Mater 2005, 17, 967.